International Journal of Fluid Machinery and Systems
Vol. 5, No. 2, April-June 2012

DOI: http://dx.doi.org/10.5293/IJFMS.2012.5.2.049
ISSN (Online): 1882-9554

Original Paper

Influence of a weak superposed centripetal flow in a rotor-stator system for several pre-swirl ratios

Fadi Abdel Nour[1], Andrea Rinaldi[2], Roger Debuchy[3] and Gérard Bois[4]

[1]Department of Water Engineering,
Damascus University, Damascus, Syria. fadi_abdnour@hotmail.com
[2] Facoltà di Ingegneria, Università degli Studi di Padova,
Lungargine del Piovego, 2 – 35131 Padova, Italy. rinaldi.and@gmail.com
[3]Laboratoire Génie Civil & géo-Environnement (LGCgE- EA 4515),
Université d'Artois/FSA Béthune, F-62400 Béthune, France. roger.debuchy@univ-artois.fr
[4]Department FISE Fluid Engineering and Energy, Arts et metiers ParisTech
LML UMR CNRS 8107 Bd Louis XIV,8 59000 Lille, France. gerard.bois@lille.ensam.fr

Abstract

The present study is devoted to the influence of a superposed radial inflow in a rotor-stator cavity with a peripheral opening. The flow regime is turbulent, the two boundary layers being separated by a core region. An original theoretical solution is obtained for the core region, explaining the reason why a weak radial inflow has no major influence near the periphery of the cavity but strongly affects the flow behavior near the axis. The validity of the theory is tested with the help of a new set of experimental data including the radial and tangential mean velocity components, as well as three components of the Reynolds stress tensor measured by hot-wire anemometry. The theoretical results are also in good agreement with numerical results obtained with the Fluent code and experimental data from the literature.

Keywords: rotor-stator cavity, turbulent flow, superposed radial inflow, analytical solution.

1. Introduction

The rotating flows have been the object of many experimental, numerical or theoretical studies, because of diversity of the scopes of application. The present work deals with the scope of the turbomachinery. In the various wheels, the flow is subjected to a forced rotation.

In gas turbines, turbojets, centrifugal multistage compressors … etc., severe operating conditions expose the moving walls to high level of stress and excitation. These phenomena can lead to problems of reliability, even of destruction if they are not correctly controlled. Thus, it is crucial to provide the best possible understanding of the aerodynamic phenomena taking place in the inter-disk spacing. Of course, these geometries are complex. They are often modeled by rotating discs cavity. Such configurations are of great interest, both from mathematical and practical point of view: on one hand, theoretical solutions can be found starting from the Navier-Stokes equations. On other hand, knowledge of the dynamic fluid properties is very important for the designers.

Von Kármán [8] was the first to consider the problem of a centrifugal flow induced by an infinite disk rotating in a fluid at rest. Starting from the equations of Navier-Stokes, he obtained a system of differential equations depending on a single variable, with the assumption that the axial velocity component is independent from the radial coordinate. A numerical solution was obtained by Cochran [9]. In 1951, Batchelor [7] considered the case of a rotating disk in a rotating fluid, the rotating speed of the fluid being lower than that of the disk. He also merged the two problems and studied the flow between two parallel and coaxial infinite disks. In that configuration, he predicted the presence of a core region in solid body rotation between two boundary layers on each disk. On the contrary, Stewartson [10] concluded that there is only a boundary layer on the rotating disk, and that the flow outside this domain has no rotation speed. This controversy was followed by numerous works to verify the validity of these theories. Since, theoretical solutions were obtained, which appear in particular in the references of Owen and Rogers [11], as well as more recently in that of Poncet et al. [2].

The present work is dedicated to the rotor-stator systems in which the flow exhibits the three domains, the two boundary layers and the core region. In such configurations, the determination of the core swirl ratio K, defined by the ratio between the tangential velocity of the fluid at mid height of the cavity and that of the rotating wall at the same radial location, is essential. Indeed, the knowledge of this physical quantity allows to estimate the pressure coefficients on the device. Therefore, numerous theoretical, experimental and numerical studies concerned this subject. In the case of a cavity subjected to a centripetal superposed flow, Kurokawa and Toyokura [12] presented a theoretical model for the radial distribution of K according to the global coefficient of flow rate C_{qr}. Poncet and al.

Received September 26 2011; revised March 2 2012; accepted for publication April 2 2012: Review conducted by Prof. Hyung-Hee Cho. (Paper number O11017K)
Corresponding author: Fadi Abdel Nour, Professor, fadi_abdnour@hotmail.com

[2, 13] obtained an analytical solution for K according to a « 5⁄7 » power law of C_{qr} with the assumption that the evolution of the velocity profile in the boundary layer corresponds to the « 1⁄7 » power law by Schlichting [4]. Numerous experimental and numerical data are in very good agreement with this model which was extended to the two regimes of flows, laminar and turbulent, and to several configurations (rotor-stator systems with and without pre-swirl, effects of roughness, rotor equipped with blades…). The extension of these models in the case of an isolated cavity, i.e. a cavity not subjected to any superposed flow, always indicates that the flow structure corresponds to the solid body rotation with K constant, as predicted by the theory of Batchelor [7]. The experiments performed by Itoh et al. [14] corroborate this prediction as a constant core swirl ratio equal to 0.43 was found in the case of an enclosed cavity. They also have shown that both turbulent regime, near the periphery, and laminar flow, closer to the axis, can coexist. The value of the core swirl ratio is not universal: Owen and Rogers [11] found a theoretical value equal to 0.382 in the case of infinite disks, Szeri and al. [15] obtained 0.313 in a system rotor-stator with a large clearance, this last result being also obtained by Dijkstra and van Heijst [16]. When the cavity is opened to the atmosphere at the periphery, D'Haudt [17] showed that the peripheral layout of the system has a strong influence on the flow properties in the case of an isolated cavity. The solid body rotation was not always observed depending on the pre-swirl velocity level, defined by the core swirl ratio at a radial coordinate equal to the rotor outer radius.

When the rotor-stator cavity is subjected to a centripetal forced flow, Debuchy [18] has shown that the superposed inflow has no major influence near the periphery, but has major effects near the axis. However, the influence of the peripheral conditions was not investigated. It is what the authors suggest as a complement in the present paper, starting from the same analytical approach as in Debuchy et al. [1, 5 and 19] and Abdel Nour et al. [6]. The objective is to succeed in modeling the radial exchanges of fluid outside the two boundary layers and to take into account the level of pre-swirl velocity of the fluid at the periphery of the cavity.

The first part of the paper deals with the analytical solutions obtained for the radial distribution of the core swirl ratio K. These solutions are based on new assumptions and bring to light interesting properties of flow, which require to be validated. The experimental set-up and measurement techniques are detailed in the second part of the paper. This part also includes details of numerical simulation setting. The analysis of the results, the comparison of the different approaches, and the validation of the model is the object of the next part. The use of the model requires the adjustment of constants. In this validation process, the authors propose empirical laws which are the most general possible. The last part summarizes the main concluding remarks of this study.

2. Theoretical approach

The studied flow occurs in an annular cavity limited by two parallel and coaxial discs. The disc located at $z = 0$, the radius of which is R, rotates with a constant angular velocity Ω (called rotor). A central hub attached to the rotor, represents the axis of real turbomachinery and avoids, from a theoretical point of view, the singularity at $r = 0$. The disc at $z = H$, is fixed (called stator). The rotor radius may be slightly different from that of the stator $(R + \Delta R)$. It is assumed that the flow is stationary and axisymmetric. The fluid is incompressible and isothermal. The cavity is opened near the axis and connected to a vacuum system in order to generate a superposed centripetal flow, the volume rate of which being q (Fig. 1).

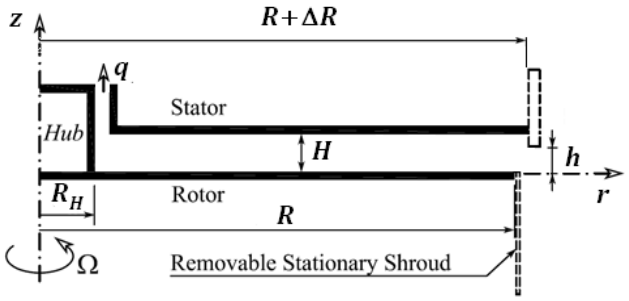

Fig. 1 Sketch of the rotor-stator cavity

For such a configuration, the main dimensionless parameters are the gap ratio of the cavity G and the Reynolds number Re, which can be replaced by the Ekman number Ek, and the Rossby number Ro. These parameters are defined by:

$$G = \frac{H}{R} \ll 1\ ;\ \ Re = \frac{\Omega R^2}{\nu} \gg 1\ ;\ \ \ Ek = \frac{1}{G^2 Re} \ll 1\ ;\ Ro = \frac{q}{2\pi\,\Omega\,R^3\,G} \ll 1 \tag{1}$$

This work focuses on the regime "IV" of the classification proposed by Daily & Nece [3] in which the flow is turbulent and presents two boundary layers separated by a core region. The authors also assume that the Rossby number is small.

Later on, the equations will be written using the following dimensionless variables:

$$r^* = \frac{r}{R}\ ;\ \ z^* = \frac{z}{GR}\ ;\ v_r^* = \frac{v_r}{\Omega r}\ \ ;\ \ v_\theta^* = \frac{v_\theta}{\Omega r}\ ;\ v_z^* = \frac{v_z}{\Omega r}\ \ ;\ \ P^* = \frac{p - p_{atm}}{\frac{1}{2}\rho\Omega^2 R^2}\ \ \ , \tag{2}$$

where v_r, v_θ and v_z represent respectively the radial, tangential and axial components of the mean velocity, and p the static pressure on the stator.

As the cavity is opened to the atmosphere, it is necessary to consider the dimensionless parameters related to the peripheral geometry of the system. Of course, it is difficult to list all these parameters: they can be related to the difference of disc radii ΔR,

wall thickness of the stationary and rotating wall, and the presence or not of shroud... Recent work [19] showed that these parameters can be replaced by one, the pre-swirl ratio K_p defined by:

$$K = v_\theta^* \left(r^*,\ z^* = \frac{1}{2}\right)\ ;\ K_p = K(r^* = 1), \tag{3}$$

where K represents the dimensionless tangential velocity at mid-high of the gap of the cavity.

In the central core, where it is assumed that the flow is governed only by the centrifugal effects and that the turbulence is neglected, the equations of the flow are:

$$\frac{1}{r^{*2}}\frac{\partial(r^{*2}v_r^*)}{\partial r^*} + \frac{1}{G}\frac{\partial v_z^*}{\partial z^*} = 0\ ;\quad \frac{dP^*}{dr^*} = 2r^*K^2\ ;\quad \frac{\partial P^*}{\partial z^*} = 0 \tag{4}$$

The static pressure P^* and the tangential velocity v_θ^* are independent of the dimensionless axial position z^*. The radial equilibrium equation (the second relation in eq. (4)) does not provide an analytical law for K.

It is necessary to obtain additional information by conducting a comprehensive review of the radial exchange of fluid. So far, the equilibrium is based only on boundary layers circulations. Thus, as mentioned in the introduction, Poncet et al. [2, 13] obtained an analytical solution for connecting K and C_{qr} according to a power law "$5/7$", assuming that the evolution of velocity profiles in boundary layers is the power law "$1/7$" mentioned by Schlichting [4]. This analytical law is:

$$K = 2\ \left(a_1\ C_{qr} + b_1\right)^{5/7} - 1\ ;\ C_{qr} = Re^{1/5} q\ r^{*-13/5}/(2\pi\Omega\ R^3), \tag{5}$$

where a_1 and b_1 are constants.

This solution, which was the subject of numerous publications, will be used as comparison reference for the validation of the present modeling. The starting point is based on the estimation of the dimensionless flow rate circulating inside the rotor and stator boundary layers, denoted respectively q_R^* and q_S^*, as in reference [19]. q_R^* and q_S^* are deduced from the stationary solutions valid for fixed and rotating infinite discs, summarized in Owen & Rogers [11]. In addition, the dimensionless volume flow rate outside the boundary layers q_C^* is also considered:

$$q_R^* \propto K_B^{\frac{4}{5}}(r^{*2}Re)^{\frac{4}{5}}\ ;\ q_S^* \propto K^{\frac{4}{5}}(r^{*2}Re)^{\frac{4}{5}}\ ;\ q_C^* \propto \left(f\left(C_{qC}\right) - 1\right) K^{\frac{4}{5}}(r^{*2}Re)^{\frac{4}{5}} \tag{6}$$

Several functions $f\left(C_{qC}\right)$ have been tested in Debuchy et al. [5], the best results, whether there is a superposed flow or not, being obtained with $f\left(C_{qC}\right) = exp\left(\varphi_1\ C_{qC}\right)$, where φ_1 is a constant. For a cavity with superposed centripetal flow, it has been shown in [5] that C_{qC} is proportional to the dimensionless flow parameter C_{qr}. Replacing eq. (6) in the global conservation of mass equation $q_S^* + q_C^* - q_R^* = q^*$ gives the following laws:

$$K^{\frac{4}{5}} = \frac{a_2\ C_{qr} + B_2}{e^{\left(\frac{4}{5}\varphi_2\ C_{qr}\right)}} \tag{7a}$$

$$K^{\frac{4}{5}} = \frac{A_2\ r^{*-13/5} + B_2}{e^{\left(\frac{4}{5}\phi_2\ r^{*-13/5}\right)}}\ ;\quad a_2 = \frac{A_2}{C_{qp}}\ ;\quad \varphi_2 = \frac{\phi_2}{C_{qp}} \tag{7b}$$

In the last relation, a_2, B_2 and φ_2 are constants and C_{qp} is the peripheral value of C_{qr}. Consequently, C_{qp} is related to some classical dimensionless parameters as following: $C_{qp} = Ro\ G\ Re^{1/5}$. Equation (7a) represents the variation of K as a function of C_{qr}, while eq. (7b) is useful to represent the radial distribution of K.

Considering the case of cavity with a very low superposed flow rate, so that $C_{qr} \to 0$, the function $exp\left(\frac{4}{5}\ \varphi_2 C_{qr}\right)$ can be replaced by its first order Taylor expansion. Consequently, eq. (7a) and eq. (7b) become:

$$K^{4/5} = \frac{a_2\ C_{qr} + B_2}{1 + \frac{4}{5}\ \varphi_2 C_{qr}} \tag{8a}$$

$$K^{4/5} = \frac{A_2\ r^{*-13/5} + B_2}{1 + \frac{4}{5}\ \phi_2 r^{*-13/5}} \tag{8b}$$

Equation (8a) which leads to obtain K as a function of dimensionless flow parameter C_{qr} can be compared to the law (5) proposed by Poncet et al [2].

3. Experimental apparatus and numerical procedure

The test rig is for the most part identical to that detailed in [19]. The authors therefore do recall the main features.

The cavity is limited by two parallel and coaxial discs separated by an adjustable distance H. The rotor of radius $R = 0.375\ m$ combined with a central hub the radius of which is $R_H = 0.09\ m$. Both are driven by an engine equipped with frequency inverter, which achieves the maximum angular speed rate of $\Omega = 209\ rad/sec$ (i.e. $2000\ rpm$). In this study, the

radius of the two discs is the same ($\Delta R = 0$). There is neither stationary shroud surrounding the rotor as in [20] nor a shroud that obstruct partially the periphery of the cavity ($h = H$). The main difference with the test rig described in [20] is located in the central part, which is here connected to a vacuum device to test the effect of a weak superposed radial inflow. A control valve and a normalized diaphragm are placed between the cavity and the ventilator. The flow is determined by measuring the differential pressure upstream and downstream of the diaphragm, using a micro-electronic manometer. The total closure of the valve isolates the cavity.

In the present study, tangential and radial mean velocity components as well as three components of the Reynolds stress tensor are measured by hot wire anemometry. The probe used is identical to that described in [19]. It consists of two wires of 5 microns in diameter, oriented at $90°$ with respect to each other, located in a plane perpendicular to the axis of the probe itself. The probe is introduced into the cavity through holes in the stator, located at dimensionless radial positions where $0.427 \leq r^* \leq 0.976$. The probe axis is always directed along z coordinate so that the two wires remain parallel to the planes of discs. The type of probe and its positioning in the cavity are based on the assumption that the axial component of the velocity is neglected in comparison with the two other velocity components. The measurement of the two effective velocities allows, after calculation, to obtain the radial v_r and tangential v_θ mean velocity components, as well as the three components $\overline{v_r'^2}$, $\overline{v_\theta'^2}$ and $\overline{v_r'v_\theta'}$. The static pressure on the stator is measured with a pressure sensor type differential Honeywell MP120 type connected to pressure taps located on the stator. The accuracy is estimated to be $\pm 2\%$ or ± 1 Pa. A schematic diagram of the experimental set-ups is presented in Fig.2 and the experimental conditions are summarized in Table 1.

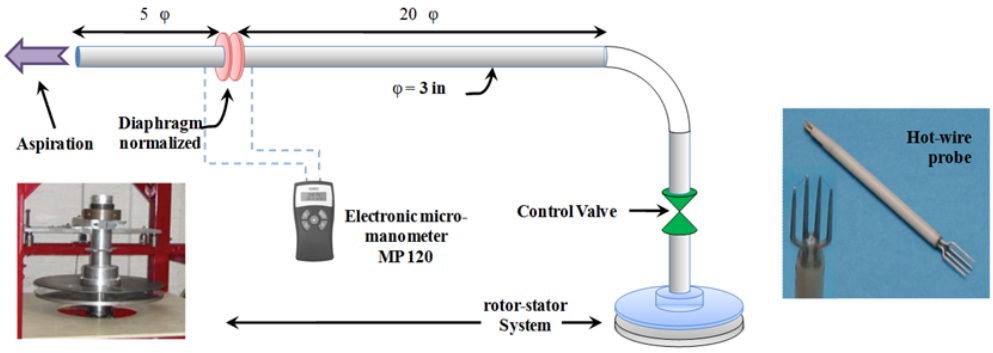

Fig. 2 Experimental apparatus

Table 1 Conditions of experiments

Symbols	G	$10^{-6} \times Re$	$10^3 \times C_{qp}$	K_p	a_2	φ_2
■	0.053	1.03	4.84	0.120	27.3	38.7
□		1.03	7.26	0.130	21.6	28.8
■		1.03	9.08	0.150	20.2	23.9
▲		1.47	3.63	0.120	31.7	45.0
△		1.47	5.45	0.120	25.3	35.9
▲		1.47	6.81	0.125	22.1	30.3
×		1.95	2.90	0.120	34.8	49.3
×		1.95	4.36	0.120	29.0	41.1
×		1.95	5.44	0.120	25.3	35.9
●	0.08	1.03	7.26	0.090	14.9	26.6
○		1.03	9.68	0.090	10.0	17.8
◆		1.47	5.45	0.080	18.0	35.3
◇		1.47	7.27	0.080	12.8	25.1
◆		1.47	9.08	0.085	10.1	18.8
+		1.95	4.36	0.075	20.9	43.2
+		1.95	5.81	0.075	15.7	32.3
+		1.95	7.26	0.075	11.7	24.2

In addition, numerical simulations have been carried out using the FLUENT 6.1 code in order to have a better understanding of the flow properties. In the present work, only the test cases corresponding to $G = 0.08$ were investigated. 2D steady and axisymmetric simulations solving RANS (Reynolds Averaged Navier Stokes) equations in the fluid domain are carried out. Three turbulence models have been tested: $k - \omega$, $k - \omega\ SST$ and RSM model. The meshes have been generated with GAMBIT 2.3. Two grids were tested in order to check any eventual influence of the discretization, the first one with 7985 cells and 5528 nodes, the second one with 15836 cells and 12635 nodes. The rotor being unshrouded, the rotating wall external to the cavity drives the fluid in the radial direction by centrifugal effect. This is the reason why the computational domain must include the area located below the rotor where a wall type condition is applied. The area located above the stator has been withdrawn from the computational domain because it has negligible effect on the peripheral flow at $r^* = 1$. It is the reason why a stationary casing

around the stator has been modeled. Fig. 3 also gives details of the mesh near the periphery of the cavity. The vertical lines inside the cavity correspond to radial locations where the numerical results have been extracted. The geometrical model includes the rotating hub in the central part of the discs and an external domain extent at the periphery of the cavity (Fig. 3). This domain extent is a key feature to obtain the correct level of pre-swirl in this kind of problem. Of course, the influence zone of the rotating disk is not known a priori. At the lower, upper and external boundaries, uniform pressure conditions have been imposed. Regarding the convergence criteria, an absolute control on the residuals was set with a value of 10^{-5} for each residual as well as a maximum number of iterations fixed on 2000. Mainly the iterations were stopped by the second one. For each test case, it was verified that there were no changes in the numerical results with up to 4000 or 6000 additional iterations.

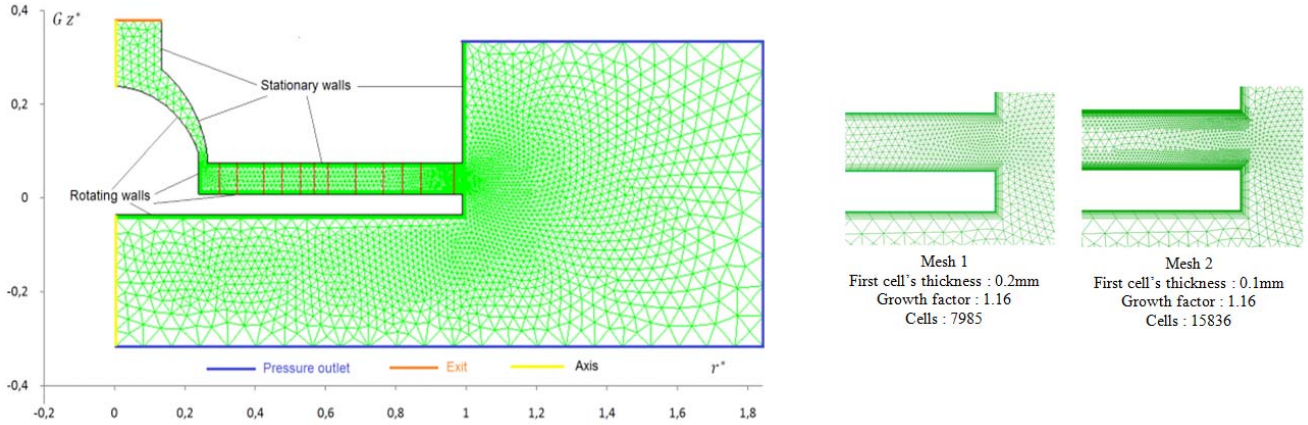

Fig. 3 Computational domain and boundary conditions

4. Results and discussion

The first part of the discussion focuses on the general properties of the flow. It is based on the analysis of the profiles of the three dimensionless mean velocities v_r^*, v_θ^* and $, v_z^*$ as well as the three dimensionless components of the Reynolds stress $\overline{v_r'^2}^*$, $\overline{v_\theta'^2}^*$ and $\overline{v_r' v_\theta'}^*$, plotted in Fig. 4. All dimensionless quantities are related to the local velocity of the rotating wall. The present test case corresponds to the following values of the dimensionless parameters: $Re = 1.95 \times 10^6$, $G = 0.08$ and $Ro = 4.03 \times 10^{-3}$. Both numerical and experimental results are displayed for four radial locations, from $r^* = 0.880$, i.e. near the periphery of the cavity, to $r^* = 0.480$. Let us mention again that the axial velocity components could not be obtained by hot-wire anemometry used technique.

Various aspects emerge. The dimensionless tangential velocity profiles v_θ^* plotted versus z^* clearly show that there is a core region separated by two boundary layers near the walls. In the core region, the axial gradient of v_θ^* is almost zero, which indicates that v_θ^* is only function of the radial position. This is in accordance with the radial and axial equilibrium equations $\frac{1}{2}\frac{dP^*}{dr^*} = r^* v_\theta^{*2}$ and $\frac{\partial P^*}{\partial z^*} = 0$. This observation is valid for both experimental and numerical results. Uppermost it is highlighted the concordance between the two different analysis approaches, as experimental and numerical data show the same types of curves. At first, it can be checked on the tangential velocity profiles at $r^* = 0.880$ that the level of pre-swirl velocity is correct for each turbulence model. Then, it is observed that the numerical results with the $k-\omega$ turbulence model greatly overestimate the measured data when approaching the axis. On the other side, the numerical results with $k-\omega\ SST$ and RSM models are in very good agreement with experiments. It seems that the RSM model is more appropriate in the upper half part of the cavity, on the stator side ($z^* \geq 0.5$), whereas the best curve in the lower one of it ($z^* \leq 0.5$), corresponds to the $k-\omega\ SST$ model. Nevertheless, both $k-\omega\ SST$ and RSM models are a good level of closure for this type of flow.

The dimensionless radial velocity profiles v_r^* plotted versus z^* clearly show that a radial exchange of fluid occurs outside the two boundary layers. v_r^* is not exactly zero as when the cavity is not subjected to any radial inflow rate and the fluid rotates as a solid body. This justifies the use of the function $f(C_{qC})$ in eq. (6). The profiles clearly indicate that the fluid goes radially inward the cavity on the stator side ($z^* \geq 0.4$) whereas it is ejected under the centrifugal effects of the rotating wall for $z^* \leq 0.4$. Generally speaking, the numerical results are not in very good agreement near the periphery of the cavity. The agreement is much better for the other radial locations, especially in the core region at $r^* = 0.533$ and $r^* = 0.480$. This means that it is more important to get the correct level of pre-swirl velocity, rather than the radial velocity profile at the periphery of the cavity in order to succeed in numerical simulation. The authors do not pay attention to the discrepancies between numerical and experimental results in the stator boundary layers. Indeed, measurements near the wall are very difficult to be performed because of the holes for the probe.

The dimensionless axial velocity profiles show that this component is very low, at least 10 times smaller than the tangential component. This component is always negative, which indicates that the rotor has a pumping effect of the fluid. The axial velocity component reaches its maximum value (in absolute value) when the radial velocity is zero.

Comparison between numerical results (using the RSM model) and experimental data for the three Reynolds stress components are also displayed in Fig. 4 at one radial location $r^* = 0.480$. The cross component is weak compared to the two

normal components, but generally speaking the turbulence intensities are very weak. Experimental data show that the turbulence is not mainly concentrated in the boundary layers because the $\overline{v_r'^2}^*$, $\overline{v_\theta'^2}^*$ and $\overline{v_r'v_\theta'}^*$ profiles slightly vary with the axial position. Large discrepancies are observed between the computational results and the experiments in the rotor boundary layer, where the turbulence intensities are slightly overestimated by the RSM model.

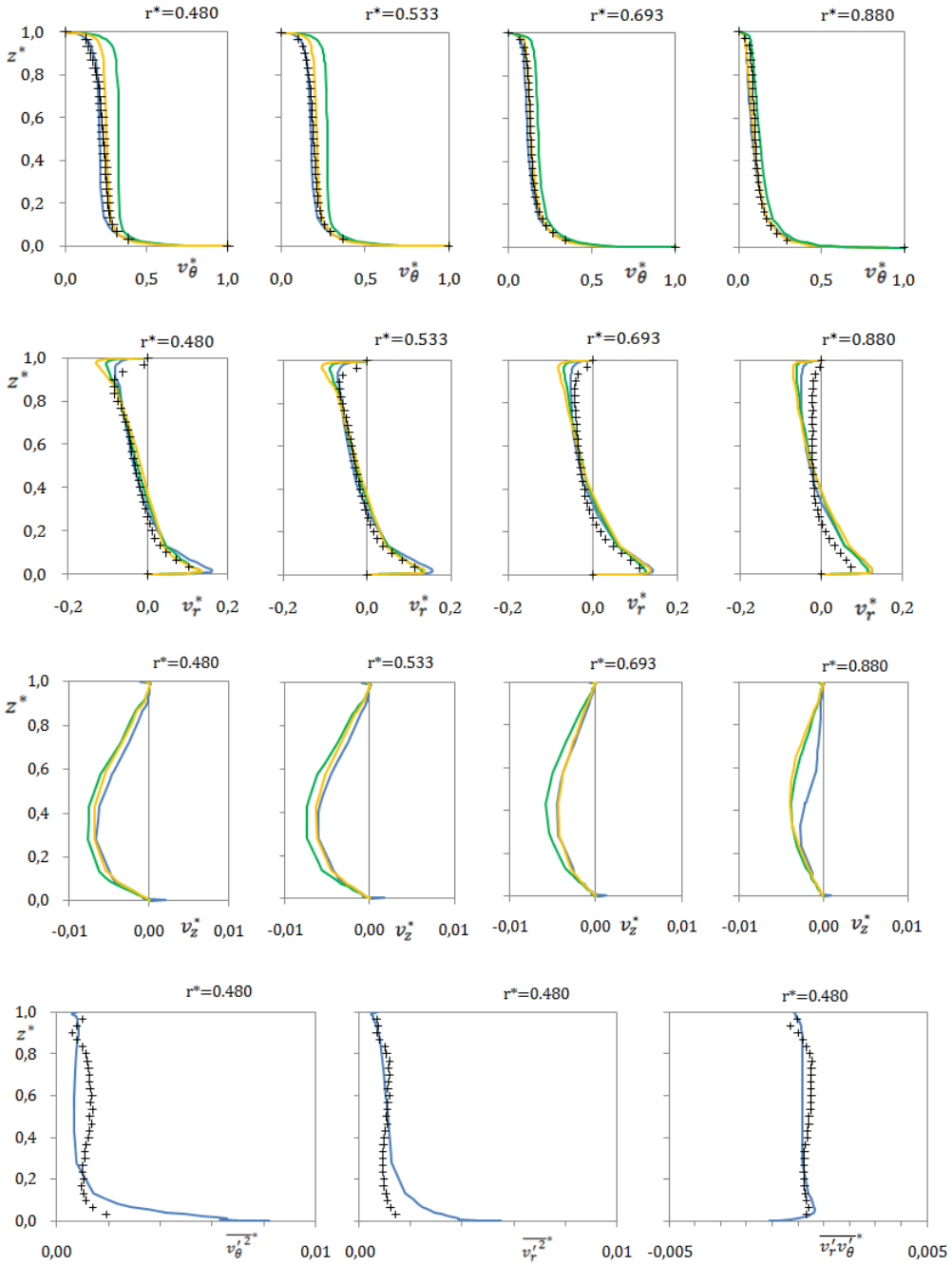

Fig. 4 Comparison between experimental and numerical results
$Re = 1.95 \times 10^6$, $G = 0.08$, $Ro = 4.03 \times 10^{-3}$
Experimental results: ✚ ; Numerical results: $k\omega$ model , $k\omega\ SST$ model , RSM model

In a second step, it is checked that the first order Taylor expansion of $f(C_{qC}) = e^{\left(\frac{4}{5}\varphi_2 C_{qr}\right)}$ introduced in eq. (7) can be used in the case of a cavity subjected to a small radial superposed flow. Figure 5 shows a comparison between the theoretical eq. (5) proposed by Poncet et al. [2], and the present eq. (7a) and eq. (8a). The differences between the curves are very small for $C_{qr} \leq 0.20$, which indicates that eq. (7a) is valid, and that eq. (8a) can replace eq. (7a) for smaller values C_{qr}. However, the results deduced from eq. (7a) are in very good agreement with the experiments when $C_{qr} > 0.20$, while the results deduced from the simplified solution (7) are very close to the law proposed by Poncet et al. [2] for positive values of C_{qr} below 0.35.

The comparisons are based only on data from reference [2]. An important conclusion in Poncet et al. [2] is that all experimental data fits on a single curve, whatever are the values of the dimensionless parameters G, Re and Ro. This conclusion is

no longer valid for the experimental results in the present work. The reason is that the cavity is completely opened to the atmosphere at the periphery with the consequence that the pre-swirl velocity of the fluid is five times lower than in Poncet et al. [13] or Owen and Rogers [11]. Figure (5b) shows that the overall results do not fit a single type curve $K = f(C_{qr})$.

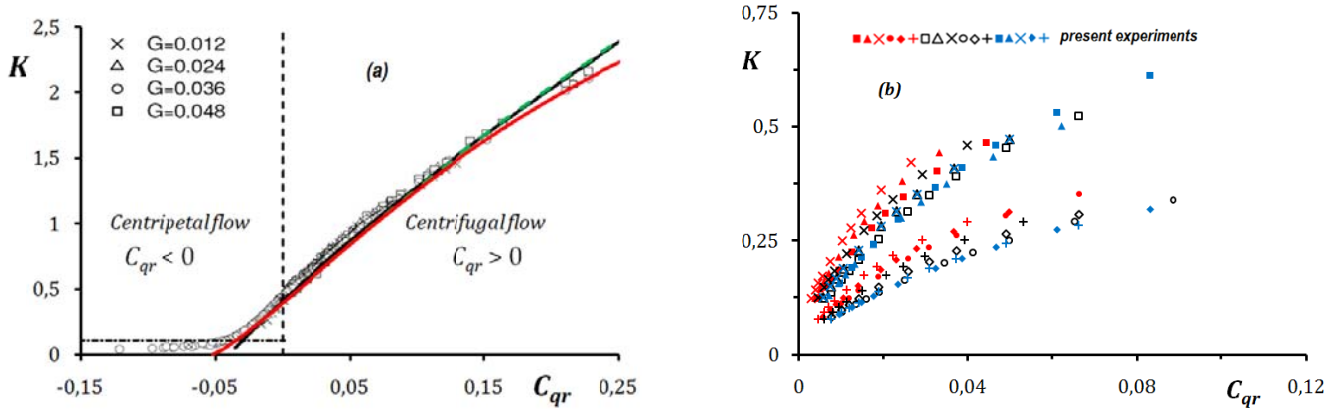

Fig. 5 Evolution of K versus C_{qr}
(a) comparison with results from [2] – (b) present experimental results
——— eq. (5) with $a_1 = 5.9$ and $b_1 = 0.63$
——— eq. (7b) and – – – eq. (8b) with $a_2 = 9.15$, $B_2 = 0.40$ and $\varphi_2 = 1.87$

It is therefore of major importance to introduce the explicit boundary condition $K = K_p$ on $r^* = 1$, so that eq. (8a) and eq. (8b) become respectively:

$$\left(\frac{K}{K_p}\right)^{4/5} - 1 = \left(a_2\, K_p^{-4/5} - \frac{4}{5}\varphi_2\right)\left(\frac{C_{qr} - C_{qp}}{1 + \frac{4}{5}\varphi_2 C_{qr}}\right) \tag{9a}$$

$$\left(\frac{K}{K_p}\right)^{4/5} - 1 = \left(A_2 K_p^{-4/5} - \frac{4}{5}\phi_2\right)\left(\frac{r^{*-13/5} - 1}{1 + \frac{4}{5}\phi_2 r^{*-13/5}}\right) \tag{9b}$$

The validation of eq. (9) requires adjustment of constants for each test case. Generally speaking, the value of C_{qp} is computed knowing G, Re and Ro. The value of the pre-swirl ratio is obtained from tangential velocity profile at $r^* = 0.976$. Then the values of the constants a_2 and φ_2 are adjusted in order to obtain the best agreement between the experimental (or numerical) and theoretical radial distributions of K. All of the adjusted values are given in Table 1. The authors also checked that the theoretical curve K versus C_{qr} deduced from eq. (8a) is also in good agreement with the experimental (or numerical) results. The empirical relationships relating the values a_2 and φ_2 to the dimensionless parameters C_{qp} and K_p can be obtained from all the experimental data (Fig. 6):

$$a_2 = 50 \times \mathrm{e}^{-15\times\frac{C_{qp}}{K_p}} \quad ; \quad \varphi_2 = 0.26 \times \frac{a_2}{K_p^{4/5}} = \frac{8.5}{K_p^{4/5}} \times \mathrm{e}^{-15\times\frac{C_{qp}}{K_p}} \tag{10}$$

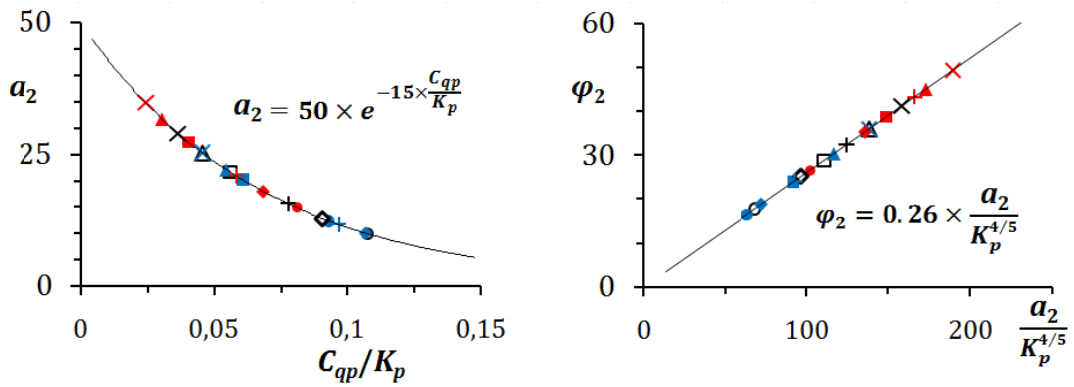

Fig. 6 Empirical laws for a_2 and φ_2.
present experiments

The combination of equations (9a), (9b) and (10) gives the following analytical laws:

$$\left(\frac{K}{K_p}\right)^{\frac{4}{5}} - 1 = 3.807\ \frac{C_{qr}-C_{qp}}{C_{qr}+\frac{5}{4\varphi_2}} \quad ; \quad \left(\frac{K}{K_p}\right)^{\frac{4}{5}} - 1 = 3.807\ \frac{r^{*-13/5}-1}{r^{*-13/5}+\frac{5}{4\phi_2}} \tag{11}$$

This last empirical equation is compared to experimental results carried out by Debuchy [1]. Three test cases are retained, where the Reynolds number and aspect ratio of the cavity remain constant ($Re = 1.47 \times 10^6$ and $G = 0.08$ respectively). The other characteristics of these tests are shown in the table below the figure. The geometry of the inner part of the system (the hub, the extraction tube...) is the same as the experimental rig in the present work. The periphery of the cavity is partially obstructed by a stationary shroud the dimensionless thickness of which is $\Delta R/H = 0.27$. The aim of this comparison is to test the validity of the empirical law (11) for pre-rotation level higher than the present results.

Figure 7a shows that the theoretical radial distributions of K calculated from eq. (11) are in very good agreement with experimental results. The theoretical radial distributions of static pressure, which is obtained with the help of the second relation in eq (4), can also be predicted with a good accuracy. This result suggests that our model has good predictive ability on our test bench, whatever the experimental conditions. However, the authors found that predictions from the empirical laws (10) and (11) are not in adequacy with the experiments by Poncet et al. [2]. One reason is that our model should also take into account the geometry of the inner part of the cavity.

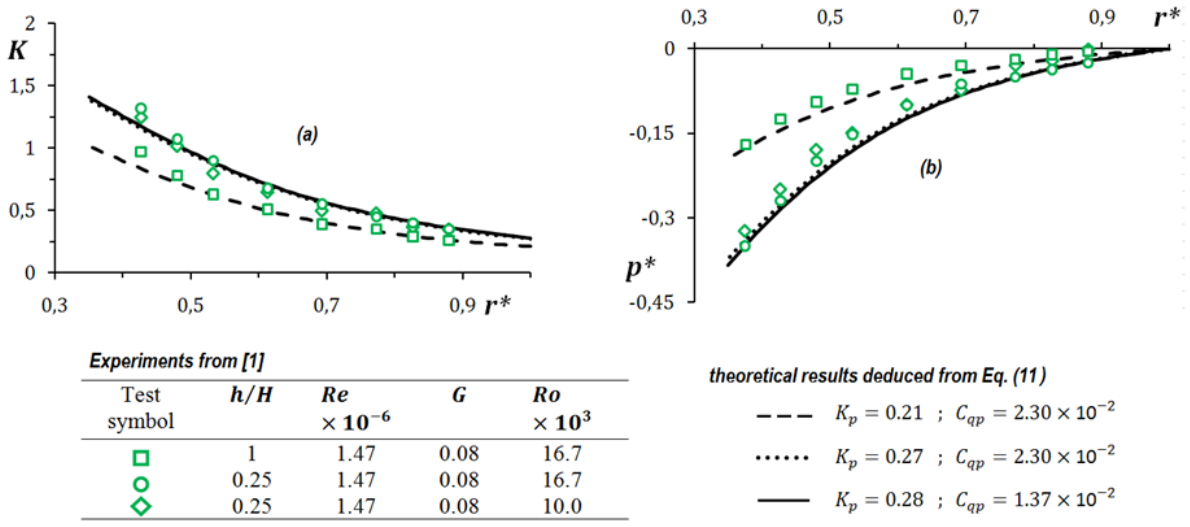

Fig. 7 Validation of eq. (11) with experimental data from [1]

The theoretical development allows to highlight other interesting properties. At first, eq. (9a) can be rewritten on the form $\left(K^{4/5} - \frac{5}{4}\frac{a_2}{\varphi_2}\right)\left(\varphi_2 C_{qr} + \frac{5}{4}\right) = \left(K_p^{4/5} - \frac{5}{4}\frac{a_2}{\varphi_2}\right)\left(\varphi_2 C_{qp} + \frac{5}{4}\right)$. This is an important result because it indicates that the quantity $\left(K^{\frac{4}{5}} - \frac{5}{4}\frac{a_2}{\varphi_2}\right)\left(\varphi_2 C_{qr} + \frac{5}{4}\right)$, which is related to the core swirl ratio K and the flow rate coefficient C_{qr}, remains constant. This constant is equal to its peripheral value $\left(K_p^{4/5} - \frac{5}{4}\frac{a_2}{\varphi_2}\right)\left(\varphi_2 C_{qp} + \frac{5}{4}\right)$ which can be determined from K_p and C_{qp}. This property clearly highlights the importance of the peripheral conditions. It has been verified that this quantity remains constant for all the experimental results performed in [20] and depicted in Table 1. Let us recall that the experiments were performed for two values of gap ratio of the cavity $G = 0.053$ and $G = 0.08$, three values of Reynolds number comprising between 1.0×10^6 and 2.0×10^6, and for a Rossby number Ro ranging from 3.0×10^{-3} to 10.7×10^{-3}.

Figure 8 shows the radial distribution of the quantity $\left(K^{4/5} - \frac{5}{4}\frac{a_2}{\varphi_2}\right)\left(\varphi_2 C_{qr} + \frac{5}{4}\right)$ for the test case corresponding to $G = 0.08$, $Re = 1.95 \times 10^6$ and $C_{qp} = 5.81 \times 10^{-3}$. According to the empirical law (10), the constants a_2 and φ_2 are respectively set to 15.7 and 32.3 (Table 1). The experimental and numerical results (with the RSM model) also show that this quantity remains constant throughout the main part of the cavity $(0.4 \le r^* \le 1)$. Only the numerical results for $r^* < 0.30$ do not check this property, which means that the function $1 + \frac{4}{5}\phi_2 r^{*-13/5}$ in our theoretical model does not give a good estimate of the exchange of fluid in the core region near the axis.

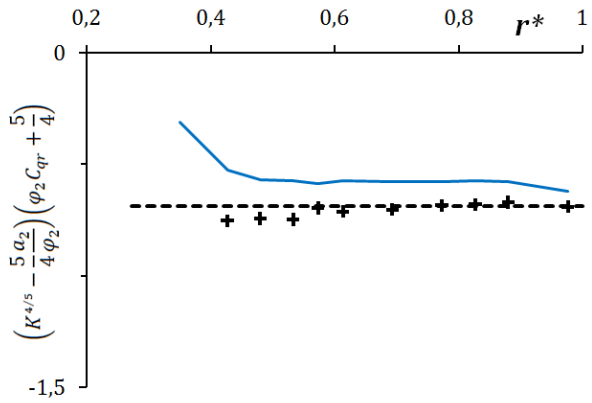

Fig. 8 Radial distribution of the quantity $\left(K^{4/5}-\frac{5}{4}\frac{a_2}{\varphi_2}\right)\left(\varphi_2 C_{qr}+\frac{5}{4}\right)$
$Re = 1.95 \times 10^6$, $G = 0.08$, $Ro = 4.03 \times 10^{-3}$
Experimental results: + ; Numerical results (RSM model): —
--- Value at $r^* = 1$: $\left(K_p^{4/5}-\frac{5}{4}\frac{a_2}{\varphi_2}\right)\left(\varphi_2 C_{qp}+\frac{5}{4}\right)$

Equation (9a) suggests that the quantity "$\left(K/K_p\right)^{4/5}-1$" is a linear function of the quantity "$\frac{C_{qr}-C_{qp}}{1+\frac{4}{5}\varphi_2 C_{qr}}$". Figure 9a shows that all the present experimental results (measurements were performed at 10 radial locations and for 17 combinations of the dimensionless parameters G, Re and Ro, i.e. 170 points) fit a single curve, for values of K_p comprising between 0.075 and 0.15 and values of C_{qp} between $2.9 \times 10^{-3}$and 12.1×10^{-3}. Figure 9b highlights the same conclusion starting from the numerical results obtained with the RSM turbulence model (computational results correspond to 11 radial locations and for 9 combinations of the dimensionless parameters G, Re and Ro, i.e. 99 points). However, some data points corresponding to the numerical results at $r^* = 0.30$ do not fit the curve. This property is valid in the main part of the cavity, except near the central hub.

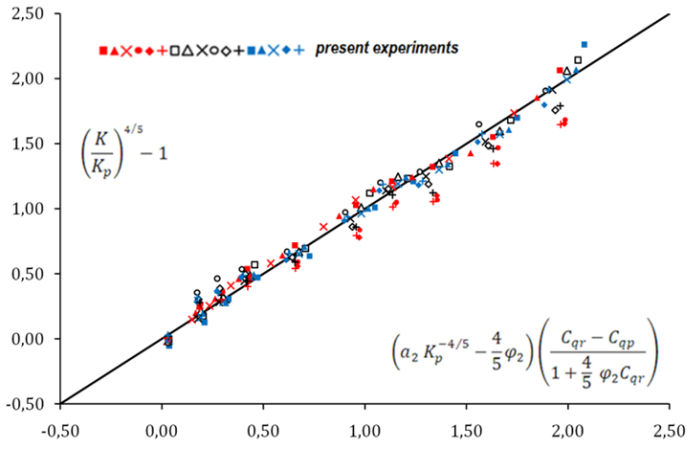

(a)

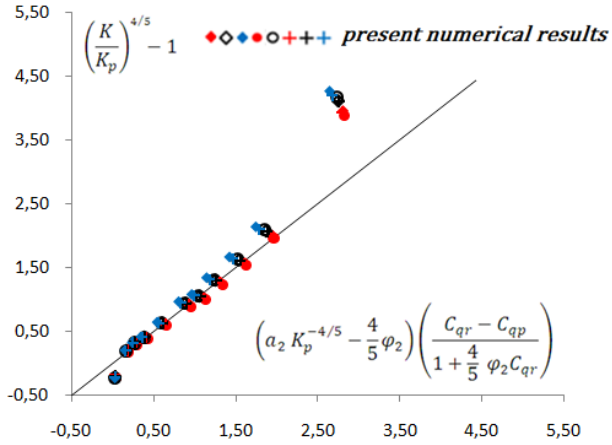

(b)

Fig. 9 Validation of eq. (9a)

5. Conclusion

This work focuses on the turbulent flow in separated boundary layers type, in a rotor-stator cavity with low superposed radial inflow. The authors propose a theoretical model based on stationary solutions of boundary layer flow on an infinite disc. Centrifuged flow in the rotor boundary layer is assumed to be identical to that generated by a rotating disc near a rotating fluid, according to von Kármán's approach. It must be compensated by a flow that circulates in both the stator boundary layer and the core region. This flow rate of compensation is determined from the Bödewadt's solution in which the authors introduce an original function in order to take into account a possible exchange outside the boundary layers. This function is supposed proportional to the dimensionless parameter C_{qr}. Under these assumptions, the global conservation of flow rates provides an analytical law for the radial distribution of the core swirl ratio K. The validation of the present model is achieved by using existing results in the literature, present experimental data, obtained by hot-wire anemometry in a specific test rig, and numerical simulations. The comparison theoretical-experimental-numerical shows that it is indispensable to take into account the radial exchange of fluid in the core region.

Nomenclature

a_1, b_1	Constants in eq. (5)
a_2, φ_2	Constants in eqs $(7a), (8a), (9a), (10)$
A_2, ϕ_2	Constants in eqs $(7b), (8b), (9b)$
B_2	Constant in eqs $(7a), (7b), (8a), (8b)$
C_{qC}	Dimensionless coefficient of flow rate in the central core, $(\propto C_{qr})$
C_{qp}	Peripheral dimensionless coefficient of flow rate,$(= Re^{1/5} q\ /(2\pi\Omega\ R^3) = Ro\ G\ Re^{1/5}\ )$
C_{qr}	Dimensionless coefficient of flow rate, $(= Re^{1/5} q\ r^{*-13/5}/(2\pi\Omega\ R^3)\ )$
Ek	Ekman number, $(= 1/(\ Re\ \ G^2))$
G	Gap ratio $(= H/R)$
h	Axial peripheral opening of the cavity [m]
H	Axial gap of the cavity [m]
K	Core swirl ratio, $(= v_\theta^*$ at $z^* = 1/2)$
K_B	Core swirl ratio for the solid body rotation
K_p	Pre-swirl ratio: core swirl ratio at $r^* = 1$
p	Static pressure on the stator [Pa]
p_{atm}	Atmospheric pressure [Pa]
p^*	Dimensionless static pressure on the stator, $\left(= p - p_{atm}/\ \frac{1}{2}\rho\Omega^2 R^2\right)$
q	Volume flow rate [$m^3.s^{-1}$]
q^*	Local dimensionless volume flow rate, $(= q/(vr))$
q_C	Volume flow rate inside the core region [$m^3.s^{-1}$]
q_C^*	Local dimensionless volume flow rate inside the core region, $(= q_C/(vr))$
q_R	Volume flow rate inside the rotor boundary layer [$m^3.s^{-1}$]
q_R^*	Local dimensionless volume flow rate inside the rotor boundary layer, $(= q_R/(vr))$
q_S	Volume flow rate inside the stator boundary layer [$m^3.s^{-1}$]
q_S^*	Local dimensionless volume flow rate inside the stator boundary layer, $(= q_S/(vr))$
r	Radial coordinate [m]
r^*	Dimensionless radial coordinate, $(= r/R)$.
R	Radius of the rotor [m]
R_H	Radius of the hub [m]
Re	Reynolds number $(= \Omega R^2/\upsilon)$
v_r	Radial velocity component [$m.s^{-1}$]
v_θ	Tangential velocity component [$m.s^{-1}$]
v_z	Axial velocity component [$m.s^{-1}$]
v_r^*	Dimensionless radial velocity component, $(= v_r/(\Omega r)\ )$
v_θ^*	Dimensionless tangential velocity component, $(= v_\theta/(\Omega r)\ )$
v_z^*	Dimensionless axial velocity component, $(= v_z/(\Omega r)\ )$
$\overline{v_i'^2}$	Turbulent correlations [$m^2.s^{-2}$], $i = r, \theta$
$\overline{v_i' v_j'}$	Turbulent correlations [$m^2.s^{-2}$], $i = r, \theta$
$\overline{v_i'^2}^*$	Dimensionless turbulent correlations, $\left(= \overline{v_i'^2}\ /(\Omega r)^2\ \right),\ i = r, \theta$
$\overline{v_i' v_j'}^*$	Dimensionless turbulent correlations, $\left(= \overline{v_i' v_j'}/(\Omega r)^2\ \right),\ i = r, \theta$
z	Axial distance from the wall of the rotor inside the cavity [m]
z^*	Dimensionless axial distance from the wall of the rotor inside the cavity, $(= z/H)$
ΔR	Difference between the rotor and stator radii [m]
Ω	Angular speed of the rotor [$rad.s^{-1}$]
ρ	Density of fluid [$kg.m^3$]
ν	kinematic viscosity of fluid [$m^2.s^{-1}$]

References

[1] Debuchy, R., Dyment, A., Muhe, H., and Micheau, P., 1998, "Radial inflow between a rotating and a stationary disc," Debuchy, R., Dyment, A., Muhe, H., and Micheau, P., 1998, "Radial inflow between a rotating and a stationary disc," European Journal of Mechanics, B, Fluids, 17(6), pp. 791-810.

[2] Poncet, S., Chauve, M.P., and Le Gal, P., 2005, "Turbulent Rotating Disk Flow with Inward Throughflow," Journal of Fluid Mechanics, 522, pp. 253-262.

[3] Daily, J.W., and Nece, R.E., 1960, "Chamber dimension effects on induced flow and frictional resistance of enclosed rotating disks," ASME J. Basic Eng., 82, pp. 217-232.

[4] Schlichting, H., 1979, "Boundary-layer theory," 7th Edn., McGraw-Hill, New-York.

[5] Debuchy, R., Abdel Nour, F., and Bois, G., 2008, "On the flow behavior in rotor-stator system with superimposed flow," International Journal of Rotating Machinery, 10, No 1155/2008/719510.

[6] Abdel Nour, F., Poncet, S., Debuchy, R., Bois, G., 2009, "A Combined analytical, experimental and numerical investigation of turbulent air flow behaviour in a rotor-stator cavity," Mécanique & Industries, 10, 3-4, pp. 195-201.

[7] Batchelor, G.K., 1951, "Note on a class of solutions of the Navier–Stokes equations representing steady rotationally-symmetric flow," Quat. J. Mech. and Appl. Math., 4, pp. 29-41.

[8] von Kármán T. 1921 "Uber laminare und turbulente reibung," Z. Angew. Math. Mech., 1 (4), pp. 233-252.

[9] Cochran. W.G. 1934 "The flow due to a rotating disk," Proc. Camb. Phil. Soc., 30: 365-375.

[10]Stewartson K. 1953 "On the flow between two rotating coaxial disks," Proc. Camb. Phil. Soc. 49, pp. 333-341.

[11]Owen J.M., & Rogers R.H., 1989 "Flow and heat transfer in rotating-disc systems, Vol. 2: Rotating cavities," Research studies press LTD.

[12]Kurokawa J., & Toyokura T., 1972 “Study on axial thrust of radial flow turbomachiner,” 2nd Int. JSME Fluid Machinery and Fluidics, Tokyo, 4-9 September. Vol. 2, p. 31.
[13]Poncet S., Chauve M.P., & Le Gal P., 2009 “Lois analytiques pour les écoulements en cavité Rotor-Stator,” Mécanique & Industries10, 3-4, pp. 195-201.
[14]Itoh M., Yamada Y., Imao S., & Gonda M. 1990 “Experiments on turbulent flow due to an enclosed rotating disk. Engineering turbulence Modeling and Experiments,” Ed. By W.Rodi, E.N. Garic, Elsevier, pp. 659-668.
[15]Szeri A. Z., Giron A., Schneider S. J., Labbe F., & Kaufman H. N. 1983 “Flow between rotating disks. Part I. Basic Flow,” J. Fluid Mech. 134, pp. 103-131.
[16]Dijkstra D. & Van Heijst G.J.F. 1983. “The flow between two finite rotating disks enclosed by a cylinder,” Journal of Fluid Mechanics, 128, pp. 123-154.
[17]D’Haudt E. 2006 “Étude expérimentale de l’influence des conditions périphériques sur un écoulement turbulent de type Rotor-Stator,” PhD Thesis, Université des Sciences et Technologies de Lille.
[18]Debuchy R. 1993 “Écoulement turbulent avec aspiration radiale entre un disque fixe et un disque tournant,” PhD Thesis, Université des Sciences et Technologies de Lille.
[19]Debuchy R., Abdel Nour F., & Bois G., 2010 “An Analytical Modeling of the Central Core Flow in a Rotor-Stator System With Several Preswirl Conditions,” J. Fluids Eng. – Vol. 132, Issue 6.
[20]Abdel Nour F. 2010 “Analyse des écoulements inter-disques en vue d'optimiser les poussées axiales dans les machines hydrauliques utilisées en station hydro-électrique,” PhD Thesis, Arts et Métiers ParisTech Lille.